Effects of a temperature-dependent viscosity on thermal convection in binary mixtures

Markus Hilt, Martin Glässl, and Walter Zimmermann*
Theoretische Physik I, Universität Bayreuth, 95440 Bayreuth, Germany
(Received 2 October 2013; published 27 May 2014)

We investigate the effect of a temperature-dependent viscosity on the onset of thermal convection in a horizontal layer of a binary fluid mixture that is heated from below. For an exponential temperature dependence of the viscosity, we find, in binary mixtures as a function of a positive separation ratio ψ and beyond a certain viscosity contrast, a discontinuous transition between two stationary convection modes having different wavelengths. In the range of negative values of the separation ratio ψ, a (continuous or discontinuous) transition from an oscillatory to a stationary onset of convection occurs beyond a certain viscosity contrast, and for large values of the viscosity ratio, the oscillatory onset of convection is suppressed.

DOI: 10.1103/PhysRevE.89.052312 PACS number(s): 66.20.−d, 47.55.P−, 47.57.−s, 44.10.+i

I. INTRODUCTION

Thermal convection occurs in fluids or gases heated from below and it is a well-known, ubiquitous phenomenon [1,2]. It drives many important processes in geoscience [3–6] or in the atmosphere [7,8], and it is a central model system of nonlinear science [9,10]. Quite often, thermal convection can be described theoretically in terms of the so-called Oberbeck-Boussinesq approximation [11] for a single-component fluid, where constant material parameters are assumed, except for the temperature-dependent density within the buoyancy term, which is the essential driving force of convection. However, in nature, the viscosity may strongly depend on the temperature, implying that models beyond the Oberbeck-Boussinesq approximation have to be used or convection takes place in fluid mixtures. Both degrees of freedom considerably affect convection, in particular, near its onset. This work discusses the combination of both effects.

For a sufficiently large viscosity contrast between the lower warmer and the upper colder region of the convection cell, related non-Boussinesq effects have be taken into account, for instance, to model convection phenomena in the Earth's mantle [6,12–22]. First studies have shown that a linear as well as a sinusoidal temperature dependence of the viscosity of a fluid may lead to a reduction in the onset of convection compared to the case of a constant viscosity [12,13,17]. In contrast, an exponential temperature dependence of the viscosity can lead either to an enhancement or to a reduction in the threshold [16,18], depending on the strength of the viscosity variation. Further, a spatially varying viscosity breaks the up-down symmetry in a convection layer, causing a subcritical convection onset to hexagonal patterns [18], and beyond the threshold, more complex convection regimes may be induced in fluids having a temperature-dependent viscosity [23].

Research on convection in binary fluid mixtures has a long tradition [24,25], with numerous applications in oceanography or geoscience [24–28], nonlinear dynamics and bifurcations [9,29–35], and, more recently, also convection in colloidal suspensions [36–41]. In binary fluid mixtures, the concentration field of one of the two constituents enters the basic equations as an additional dynamic quantity [11,42]: via the Soret effect (*thermophoresis*) [43], a temperature gradient applied to a binary fluid mixture in a convection cell causes a spatial dependence of the concentration field, which couples into the dynamical equation for the velocity field via the buoyancy term. The dynamics near the onset of convection in mixtures of alcohol and water as well as in ^{3}He-^{4}He mixtures is well investigated with a good agreement between measurements and theory [9,31]. The possibility of a stationary as well as an oscillatory onset of convection in binary-fluid mixtures, including a so-called codimension-2 bifurcation at the transition between both instabilities, caused additional attraction [9].

Although the temperature dependence of the viscosity as well as the two-component character of fluids is considered to be of importance for modeling many phenomena in planetary science [3–6,25–28], the influence of a combination of both effects onto convection is still nearly unexplored [44,45]. As turbulent convection causes a homogenization of concentrations and of the temperature field in the center of a convection cell, the impact of a combination of both effects is expected to be less significant in the turbulent regime but to be of particular importance at the onset of convection, which is the focus of this work.

In Sec. II, we present the dynamical equations and in Sec. III A, we reconsider the observation that for a one-component fluid, in the case of a linear temperature dependence of the viscosity and a small viscosity contrast, one has a reduction in the onset of convection, while there is an enhancement of the threshold for an exponential temperature dependence. The influence of a temperature-dependent viscosity on the onset of convection in a binary mixture is considered in Secs. III B and III C, both along the stationary branch as well as along the oscillatory branch, including the codimension-2 point. Most striking, we find that the oscillatory branch can be suppressed by strong viscosity contrasts. In Sec. IV, the results are summarized and discussed.

II. BASIC EQUATIONS AND HEAT CONDUCTING STATE

Compared to the common basic equations for convection in binary fluid mixtures in the Boussinesq approximation [32,34], we replace the constant viscosity by a temperature-dependent kinematic viscosity of a fluid $\nu = \nu_\infty \exp(\bar{\gamma}/T)$, whereby we assume that both components of the mixture have the same

*walter.zimmermann@uni-bayreuth.de

temperature dependence [46,47]. With the mean temperature in the convection cell, T_0, and a Taylor expansion of the exponent around T_0 up to the leading order, the viscosity takes the form

$$\nu = \nu_0\, e^{-\gamma(T-T_0)}, \tag{1}$$

where $\gamma = \bar{\gamma}/{T_0}^2$ and $\nu_0 = \nu(T = T_0) = \nu_\infty \exp(\bar{\gamma}/T_0)$. In a binary mixture, a temperature-dependent viscosity implies, via $D \sim 1/\nu$, also a temperature-dependent mass diffusion constant D:

$$D = D_0\, e^{\gamma\,(T-T_0)}. \tag{2}$$

We would like to stress that this relation does not hold in general but is appropriate when the dependence of the viscosity on the temperature is roughly identical for both components or when the concentration of the second component is very low, such that the viscosity of the mixture is almost exclusively determined by the first component. In Sec. III, we restrict our analysis to these two cases.

The basic transport equations [42] for an incompressible binary fluid mixture involve a dynamical equation for the temperature field $T(\mathbf{r},t)$, the mass fraction of the second component $N(\mathbf{r},t)$, and the fluid velocity $\mathbf{v}(\mathbf{r},t)$:

$$\boldsymbol{\nabla}\cdot\mathbf{v} = 0, \tag{3a}$$

$$(\partial_t + \mathbf{v}\cdot\boldsymbol{\nabla})T = \chi\,\Delta T, \tag{3b}$$

$$(\partial_t + \mathbf{v}\cdot\boldsymbol{\nabla})N = \boldsymbol{\nabla}\cdot\left(D\left(\boldsymbol{\nabla}N + \frac{k_T}{T_0}\boldsymbol{\nabla}T\right)\right), \tag{3c}$$

$$(\partial_t + \mathbf{v}\cdot\boldsymbol{\nabla})\mathbf{v} = -\frac{1}{\rho_0}\boldsymbol{\nabla}p + \boldsymbol{\nabla}\cdot\mathcal{S} - \frac{\rho}{\rho_0}g\hat{\mathbf{e}}_z. \tag{3d}$$

Herein,

$$\mathcal{S} = \nu(\boldsymbol{\nabla}\mathbf{v} + (\boldsymbol{\nabla}\mathbf{v})^T) \tag{4}$$

describes the stress tensor, χ denotes the thermal diffusivity of the mixture, k_T is the dimensionless thermal-diffusion ratio, which couples the temperature gradient to the particle flux and is related to the Soret coefficient S_T via $k_T/T = N(1-N)S_T$, and $p(\mathbf{r},t)$ denotes the pressure field. As in the common Boussinesq approximation, we assume that χ and $k_T/T \sim N_0(1-N_0)S_T$ are constants and the dependence of the density ρ on T and N is taken into account only within the buoyancy term, where we assume a linearized equation of state of the form [11,35]

$$\rho = \rho_0[1 - \alpha(T - T_0) + \beta(N - N_0)] \tag{5}$$

with the thermal expansion coefficient $\alpha = -(1/\rho_0)\partial\rho/\partial T$ and $\beta = (1/\rho_0)\partial\rho/\partial N$.

Equations (3) are completed by no-slip boundary conditions. For a fluid that in the z direction is confined between two impermeable, parallel plates at a distance d that are held at constant temperatures and extend infinitely in the x-y plane, the following set of boundary conditions results at $z = \pm d/2$:

$$T = T_0 \mp \frac{1}{2}\,\delta T, \tag{6a}$$

$$0 = \partial_z N + \frac{k_T}{T_0}\,\partial_z T, \tag{6b}$$

$$0 = v_x = v_y = v_z. \tag{6c}$$

In the absence of convection (i.e., for $\mathbf{v} = 0$), the time-independent—and, with respect to the x-y plane—translational symmetric heat-conducting state is given by

$$T_{\mathrm{cond}}(z) = T_0 - \delta T\,\frac{z}{d}, \tag{7a}$$

$$N_{\mathrm{cond}}(z) = N_0 - \delta N\,\frac{z}{d}, \quad \text{with} \quad \delta N = -\frac{k_T}{T_0}\delta T. \tag{7b}$$

For further analysis, it is convenient to separate this basic heat-conducting state from convective contributions setting $T(\mathbf{r},t) = T_{\mathrm{cond}}(z) + T_1(\mathbf{r},t)$ and $N(\mathbf{r},t) = N_{\mathrm{cond}}(z) + N_1(\mathbf{r},t)$. Making use of the rotational symmetry in the fluid layer, we can restrict our analysis to the x-z plane and introduce a scalar velocity potential $F(x,z,t)$ via

$$v_x = \partial_z\partial_x F, \quad v_z = -\partial_x^2 F, \tag{8}$$

with the help of which Eq. (3a) is fulfilled by construction. Rescaling distances by d, times by the vertical diffusion time d^2/χ, the temperature field T by $\chi\nu_0/\alpha g d^3$, the concentration field N by $-k_T\chi\nu_0/T_0\alpha g d^3$, and the velocity potential F by χd, all material and geometry parameters are regrouped in five dimensionless parameters: the *Rayleigh number* R (representing the control parameter), the *separation ratio* ψ (related to the Soret effect), the *Prandtl number* P, and the *Lewis number* L,

$$R = \frac{\alpha g d^3}{\chi\nu_0}\,\delta T, \quad \psi = \frac{\beta k_T}{\alpha T_0}, \quad P = \frac{\nu_0}{\chi}, \quad L = \frac{D_0}{\chi}, \tag{9}$$

are well known from common molecular binary fluid mixtures [35] and the fifth dimensionless quantity

$$\Gamma = \frac{\chi\nu_0}{\alpha g d^3}\,\gamma \tag{10}$$

characterizes the viscosity contrast $\bar{\nu}$ between the viscosity at the upper and that at the lower boundary via

$$\bar{\nu} = \frac{\nu(z=+1/2)}{\nu(z=-1/2)} = e^{\Gamma R}. \tag{11}$$

In the following, we discuss our results mainly in dependence on ψ and Γ, whereas P and L are fixed to $P = 10$ and $L = 0.01$, respectively.

Finally, by introducing a rescaled temperature deviation $\theta = (R/\delta T)\,T_1$, a rescaled concentration deviation $\tilde{N}_1 = -(T_0 R/k_T\delta T)N_1$, and a rescaled velocity potential $f = 1/(\chi d)F$ and using the combined function $\tilde{c} = \tilde{N}_1 - \theta$ instead of $\tilde{N}_1$, we obtain

$$(\partial_t - \Delta)\theta + R\partial_x^2 f = -\big(\partial_z\partial_x f\,\partial_x - \partial_x^2 f\,\partial_z\big)\theta, \tag{12a}$$

$$\partial_t c - L\boldsymbol{\nabla}\cdot(e^{\Gamma(-Rz+\theta)}\boldsymbol{\nabla}c) + \Delta\theta = -\big(\partial_z\partial_x f\,\partial_x - \partial_x^2 f\,\partial_z\big)c, \tag{12b}$$

$$\begin{aligned}\partial_t\Delta\partial_x f - P\Delta(e^{-\Gamma(-Rz+\theta)}\Delta\partial_x f) + P\psi\,\partial_x c + P(1+\psi)\partial_x\theta \\ + 2P\big[\big(\partial_z^2 e^{-\Gamma(-Rz+\theta)}\big)\partial_x^2 + \big(\partial_x^2 e^{-\Gamma(-Rz+\theta)}\big)\partial_z^2\big]\partial_x f \\ - 4P(\partial_x\partial_z e^{-\Gamma(-Rz+\theta)})\partial_x^2\partial_z f \\ = -\big(\partial_z\partial_x f\,\partial_x - \partial_x^2 f\,\partial_z\big)\partial_x f,\end{aligned} \tag{12c}$$

together with the no-slip, impermeable boundary conditions

$$\theta = \partial_z c = \partial_x f = \partial_z \partial_x f = 0 \quad \text{at} \quad z = \pm 1/2, \tag{13}$$

where, for simplicity, all tildes have been suppressed.

III. ONSET OF CONVECTION

The parameters at the onset of convection are determined by a linear stability analysis of the basic, nonconvective state $\theta = c = f = 0$, as, for instance, described in more detail in Ref. [39]. For this purpose, the linearized equations

$$\partial_t \theta = \Delta\theta - R\partial_x^2 f, \tag{14a}$$

$$\partial_t c = -\Delta\theta + L\nabla\cdot(e^{-\Gamma R z}\nabla c), \tag{14b}$$

$$\frac{1}{P}\partial_t \Delta\partial_x f = -\psi\partial_x c - (1+\psi)\partial_x\theta + \Delta(e^{\Gamma R z}\Delta\partial_x f) - 2\Gamma^2 R^2 e^{\Gamma R z}\partial_x^2\partial_x f \tag{14c}$$

are solved by a Fourier ansatz along the horizontal direction: $(\theta, c, f) = (\bar\theta(z), \bar c(z), \bar f(z))\exp(i\,k\,x + \sigma t)$. The z dependence of the fields $\bar\theta(z)$, $\bar c(z)$, and $\bar f(z)$ are expanded with respect to trivial polynomials of the lowest order, satisfying the boundary conditions in Eq. (13) orthogonalized via the Gram-Schmidt algorithm. By a projection of the linear equations onto these polynomials (Galerkin method; see, e.g., Refs. [48–50]), the dynamical equations are transformed into an eigenvalue problem. By the condition $\mathrm{Re}(\sigma) = 0$, the neutral curve $R_0(k)$ for the Rayleigh number is determined, whose minimum (R_c, k_c) at the critical Rayleigh number R_c and the critical wave number k_c determines the onset of convection. With $\omega_c = \mathrm{Im}(\sigma)$, we denote the frequency at the threshold of the oscillatory onset of convection.

A. Simple fluids ($\psi = 0$)

First, let us concentrate on the effect of an exponentially temperature-dependent viscosity on the onset of convection for one-component fluids ($\psi = 0$).

For this case, the critical Rayleigh number R_c and the corresponding critical wave number k_c are shown in Fig. 1 as a function of Γ (solid lines). Both quantities reveal a nonmonotonic dependence on Γ, similar to the results reported in Refs. [16] and [51]: while for small Γ, R_c rises compared to the case of a constant viscosity, the threshold is reduced in the limit of large Γ. This contrasts to related studies [17], where a linear temperature dependence of the viscosity has been assumed and which predict a monotonic decrease in the threshold with rising viscosity contrast. However, we can reproduce that result by a linear approximation of the exponential terms in Eqs. (12), which is also shown in Fig. 1 (dotted lines) and which clearly demonstrates the importance of terms higher than the leading linear order. The velocity potential f at the onset of convection is shown in Fig. 2 for two values of Γ. The more strongerly the viscosity varies in space, the more the center of the convection rolls is shifted towards the lower boundary and the more the fluid motion is suppressed near the upper boundary, where a highly viscous layer forms.

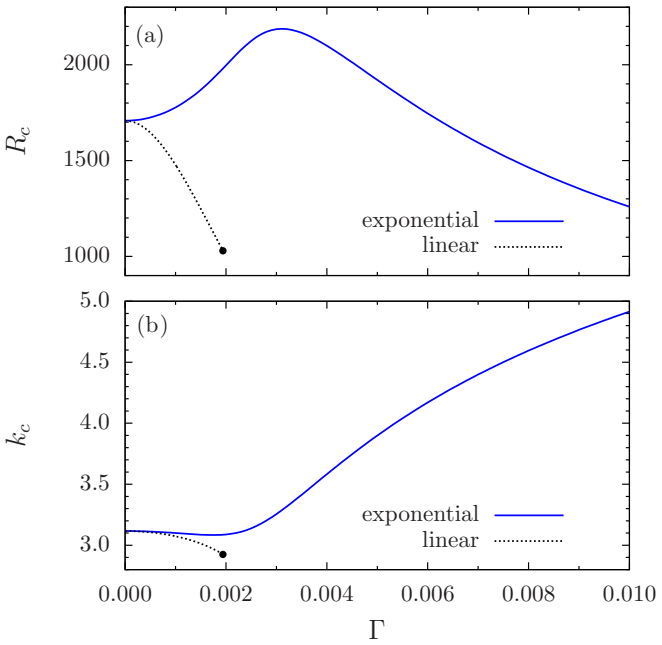

FIG. 1. (Color online) (a) The critical Rayleigh number R_c and (b) the critical wave number k_c for a one-component fluid as a function of Γ. The solid line marks the exponential temperature dependence of the viscosity; the dotted line, the linear one. The dotted line ends at $\Gamma \approx 1.941 \times 10^{-3}$ (filled black circle), where the viscosity becomes negative at the upper boundary.

B. Binary mixtures with a positive Soret effect ($\psi > 0$)

In the range of a positive Soret effect, i.e., $\psi > 0$, where the minor component of the binary mixture is driven to the colder boundary, convection sets in stationary for all Γ, just as in the case of a constant viscosity [32–35]. Figure 3 shows R_c and

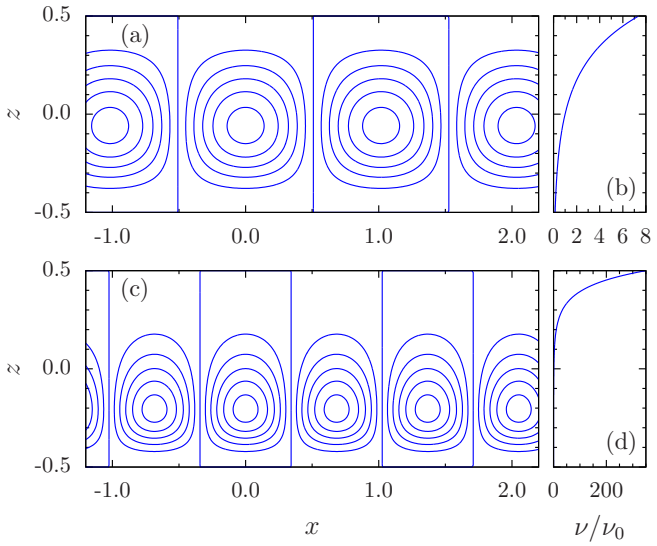

FIG. 2. (Color online) Contour lines of the velocity potential f at the onset of convection for (a) $\Gamma = 0.002$ and (c) $\Gamma = 0.008$. (b, d) Corresponding spatial dependence of the viscosity $\nu(z)/\nu_0$. Critical values are $k_c = 3.09$ and $R_c = 1997$ (a, b) and $k_c = 4.59$ and $R_c = 1464$ (c, d).

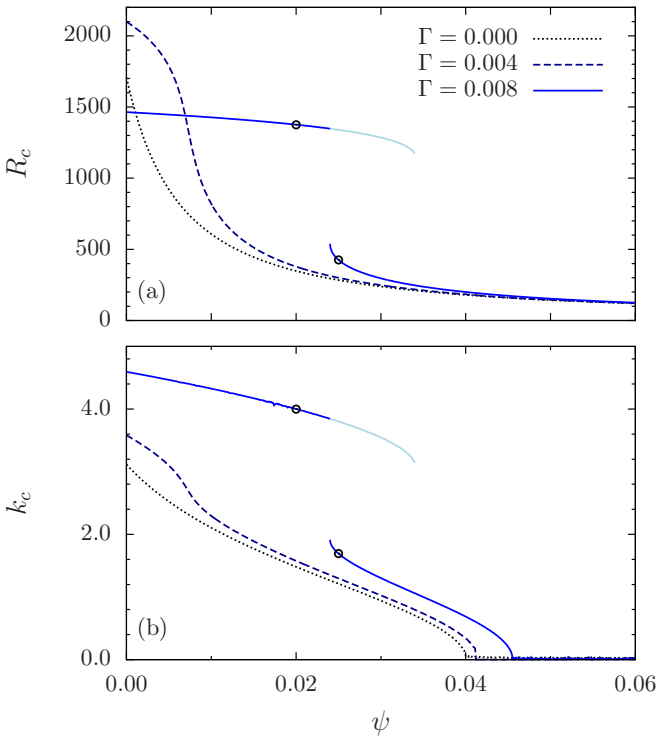

FIG. 3. (Color online) Critical values (a) $R_c(\psi)$ and (b) $k_c(\psi)$ for $\Gamma = 0.000$, 0.004, and 0.008. Circles mark those values of ψ for which neutral curves are shown in Fig. 4.

k_c as functions of ψ for two representative finite values of Γ as well as for the limiting case $\Gamma = 0$. For moderate values of Γ (dashed lines), R_c and k_c are higher than for $\Gamma = 0$ (dotted lines) and their behavior as functions of ψ, in particular, the shift of k_c towards 0 for rising values of ψ, is pretty similar to that for $\Gamma = 0$. However, for higher values of Γ (solid lines) and small ψ, the threshold is reduced compared to $\Gamma = 0$, which is similar to the case of a simple fluid as shown in Fig. 1. In addition, for large Γ, the decay of R_c as a function of ψ becomes much weaker, and most importantly, at a certain value of ψ, the threshold discontinuously jumps to much lower values, which are comparable to those for $\Gamma = 0$.

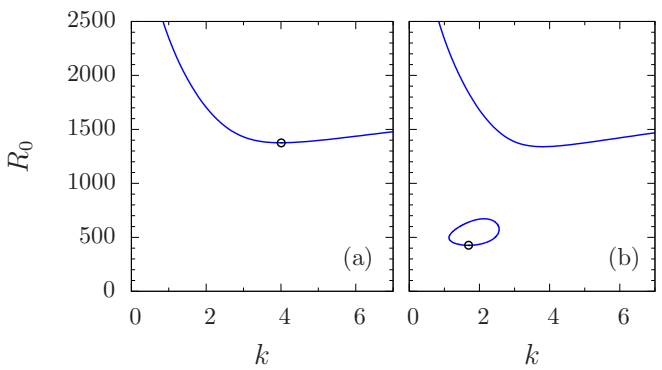

FIG. 4. (Color online) Neutral curves corresponding to the circles in Fig. 3 with (a) $\psi = 0.02$ and (b) $\psi = 0.025$ for $\Gamma = 0.008$. Circles mark the minima of the neutral curves.

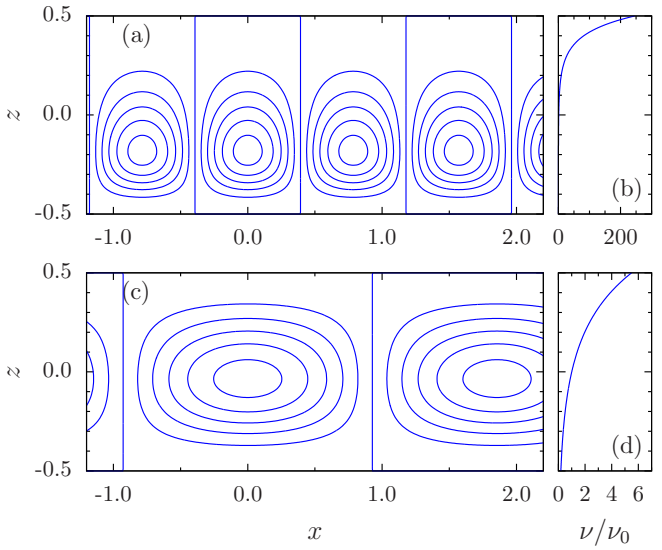

FIG. 5. (Color online) Contour lines of the velocity potential f at the onset of convection corresponding to (a) Fig. 4(a) ($\psi = 0.020$, $\Gamma = 0.008$, $k_c \cong 4.00$, $R_c \cong 1376$) and (c) Fig. 4(b) ($\psi = 0.025$, $\Gamma = 0.008$, $k_c \cong 1.69$, $R_c \cong 426$). (b, d) The corresponding decay of the viscosity.

To understand this discontinuous behavior, Fig. 4 shows the neutral curves $R_0(k)$ for two values of ψ, which are to the right or left of the jump, respectively, and which are shown by circles in Fig. 3. For the larger value of ψ [cf. Fig. 4(b)], an additional region of stationary instability forms in the (R,k) plane with a minimum at lower Rayleigh numbers, which explains the discontinuity shown in Fig. 3.

As the viscosity contrast [cf. Eq. (11)] at the onset of convection is given by the product of Γ and R_c, the jump in the critical Rayleigh number leads, for ψ close to the discontinuity, to a strong change in the viscosity contrast at the threshold. This, finally, leads to very different velocity fields at the onset of convection for values of ψ that are to the right or to the left of the jump, which is illustrated by the velocity potential in Figs. 5(a) and 5(c), respectively. For the smaller value of ψ, R_c is higher [cf. Fig. 4(a)], leading to a stronger viscosity contrast [cf. Fig. 5(b)] and therefore to a pronounced shift of the flow field towards the lower boundary [cf. Fig. 5(a)]. In contrast, for the larger value of ψ, the threshold R_c is smaller [cf. Fig. 4(b)], the viscosity contrast is much weaker [cf. Fig. 5(d)], and thus, there is only a slight shift of the convection rolls [cf. Fig. 5(c)]. Further, the different lateral extension of the role structure shown in Figs. 5(a) and 5(c) reflects the jump in k_c [cf. Fig. 3(b)].

C. Binary mixtures with a negative Soret effect ($\psi < 0$)

The most interesting effect of a strongly temperature-dependent viscosity occurs in the range of a negative Soret effect, i.e., for $\psi < 0$, where the minor component of the binary mixture is enriched at the warmer boundary: With increasing values of Γ, the divergence of the stationary instability (in the case of a constant viscosity [32–35]) vanishes. Further, beyond a certain L-dependent value of Γ, the onset of convection is no longer oscillatory for all $\psi < 0$, as is

known in the case of a constant viscosity. Instead, at strongly negative values of ψ, the oscillatory instability is replaced by a stationary one. Depending on the strength of the exponential temperature dependence of the viscosity, the transition from a Hopf bifurcation to a stationary instability with decreasing ψ can show a discontinuous or a continuous threshold behavior.

1. Discontinuous transition from an oscillatory to a stationary instability

For moderate values of Γ, the transition between the two types of instabilities is characterized by a discontinuous jump in R_c, k_c, and ω_c, as exemplarily illustrated in Fig. 6 for $\Gamma = 0.003$. The corresponding neutral curves $R_0(k)$ for different ψ are shown in Fig. 7, where dashed (red) lines indicate those parts of the neutral curves where the frequency ω is finite, while solid (blue) lines represent a stationary instability with $\omega = 0$. For small $|\psi|$, the minima of the neutral curves [dotted (green) line] belong to an oscillatory instability. However, with increasing $|\psi|$, this region transforms into an oscillatory island, which finally disappears, while the stationary branch of the curve, which shows a minimum at larger values of k, remains. In consequence, for even larger $|\psi|$, convection sets in stationarily at a higher threshold and a considerably increased critical wave number. These changes are directly reflected in the velocity potential at the onset of convection, as shown in Figs. 8(a) and 8(c): While Fig. 8(a) shows traveling waves in the regime of oscillatory instability, Fig. 8(c) displays

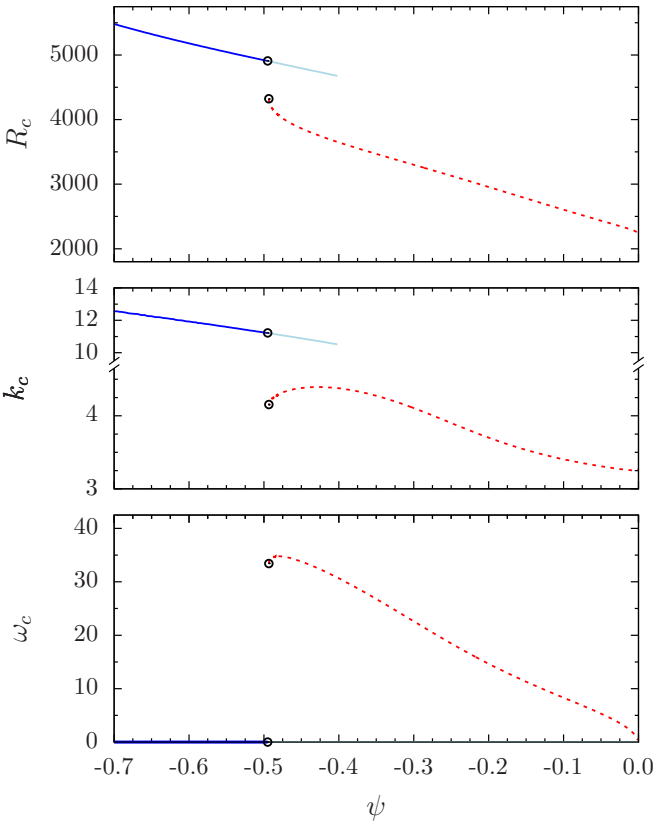

FIG. 6. (Color online) (a) Critical Rayleigh number R_c, (b) critical wave number k_c, and (c) critical frequency ω_c as functions of $\psi < 0$ for $\Gamma = 0.003$.

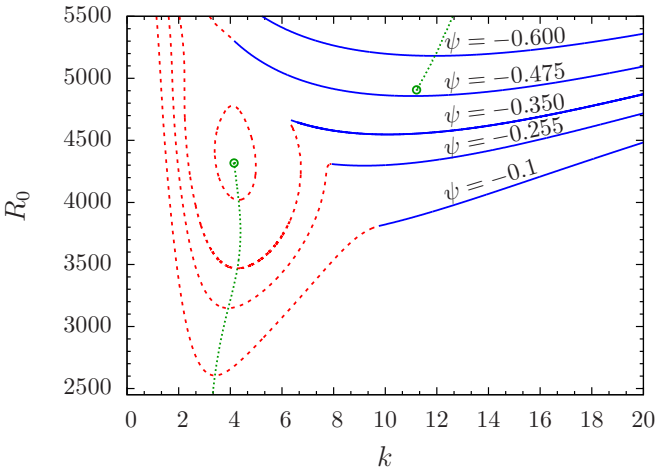

FIG. 7. (Color online) Neutral curves for $\Gamma = 0.003$ and different $\psi < 0$ as indicated. The dotted (green) line marks the position of the absolute minima of the neutral curves. At the critical value $\psi_c \cong -0.5$, the transition from an oscillatory to a stationary instability takes place. At that point, the minimum of the neutral curves shows a discontinuous jump in k_c and R_c (circles).

stationary convection rolls with a much smaller lateral width (due to the jump in k_c), which are also much more shifted to the lower boundary [due to the higher threshold and, hence, the more pronounced viscosity contrast; cf. Figs. 8(b) and 8(d)].

2. Continuous transition from an oscillatory to a stationary instability

For larger values of Γ, the transition between the Hopf and the stationary bifurcation is still characterized by jumps in the critical wave number and the critical frequency but no longer shows a discontinuity in the threshold, as illustrated in Fig. 9 for $\Gamma = 0.004$. Instead of forming an oscillatory island that,

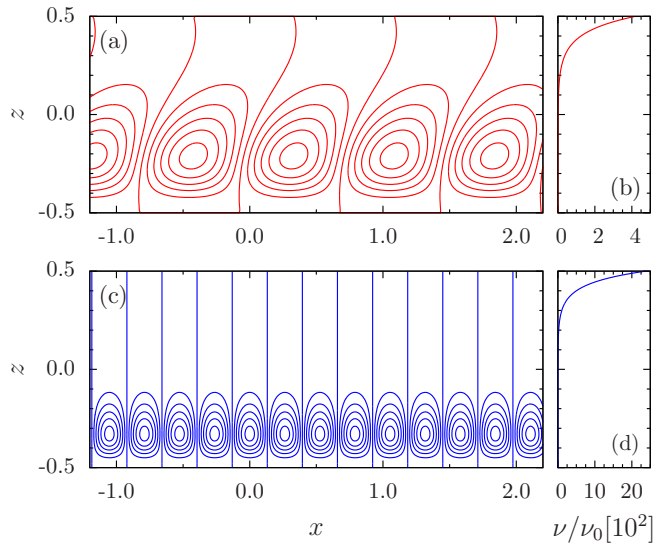

FIG. 8. (Color online) Contour lines of the velocity potential f at the onset of convection corresponding to Fig. 7 for (a) $\psi = -0.475$, $k_c \cong 4.17$, $R_c \cong 4026$ and (c) $\psi = -0.6$, $k_c \cong 11.93$, $R_c \cong 5181$. (b, d) The corresponding decay of the viscosity.

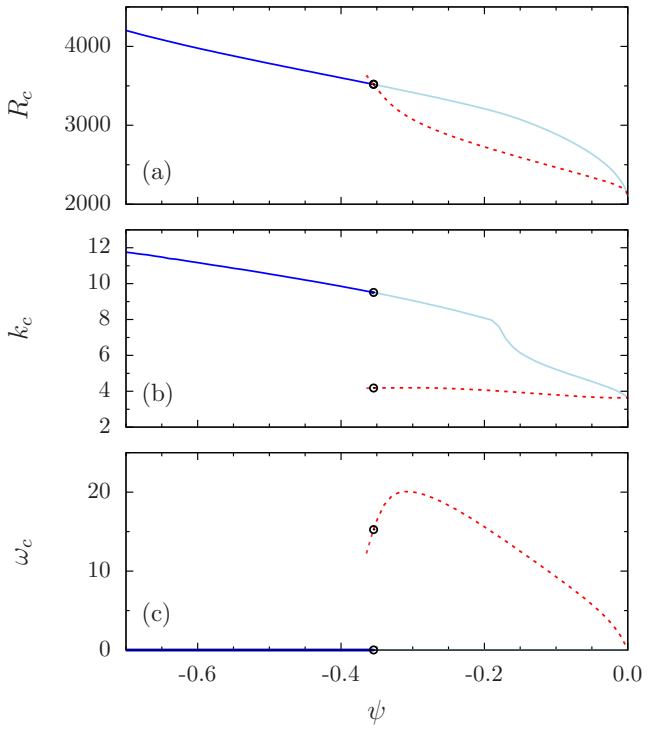

FIG. 9. (Color online) (a) Critical Rayleigh number R_c, (b) critical wave number k_c, and (c) critical frequency ω_c as functions of $\psi < 0$ for $\Gamma = 0.004$.

for rising $|\psi|$, will eventually disappear, here, as displayed in Fig. 10, for rising $|\psi|$, the minimum of the oscillatory branch of the neutral curves moves higher and higher. At

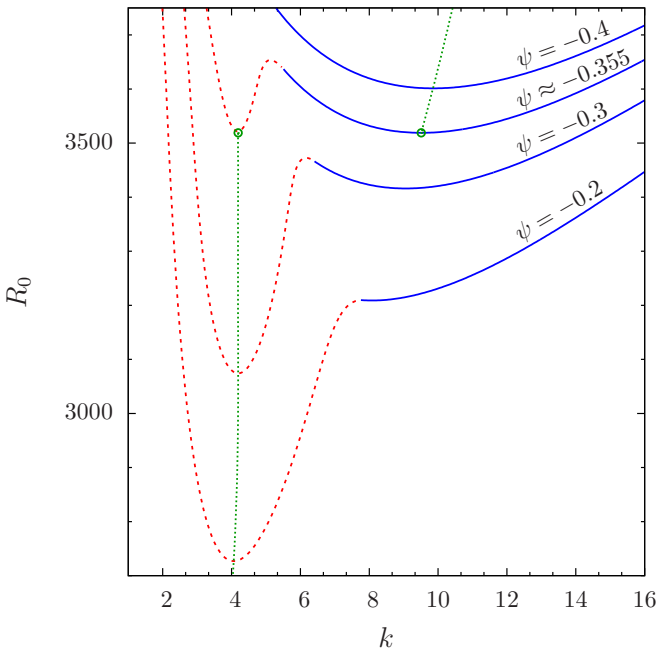

FIG. 10. (Color online) Neutral curves for $\Gamma = 0.004$ and different $\psi < 0$ as indicated. The dotted (green) line marks the position of the absolute minima of the neutral curves. At $\psi_c \cong -0.355$, the transition from an oscillatory to a stationary instability takes place and the minimum of the neutral curves shows a discontinuous jump in k_c (circles).

a certain value of ψ, the minima of the oscillatory [dashed (red) line] and stationary [solid (blue) line] branches are of equal height, and with further increasing $|\psi|$, the minimum of the stationary branch is finally lower and determines the onset of convection. The changes of the velocity potential near this new codimension-2 point are similar to those depicted in Fig. 8. The stationary branch of the critical Rayleigh number, shown in Fig. 9(a) [solid (blue) line] in the range of $\psi < 0$ is continued by the corresponding curve ($\Gamma = 0.004$) in Fig. 3(a) to the range $\psi > 0$.

A further interesting difference in the scenarios shown in Figs. 6–8 versus Figs. 9–10 is that for increasing Γ, the change from oscillatory to stationary convection takes place at a smaller value of $|\psi|$. With further increasing Γ, this trend continues, i.e., for rising strength of the exponential temperature dependence of the viscosity, the region in the parameter range $\psi < 0$, where convection sets in via a Hopf bifurcation, becomes smaller and smaller.

IV. SUMMARY AND CONCLUSIONS

The parameters at the onset of convection are determined in a binary fluid mixture where the viscosity depends exponentially on the temperature. As explicitly shown for a single-component fluid, the critical values at the onset of convection behave as a function of the viscosity difference between the lower, warmer and the upper, colder boundary differently for a linear temperature-dependent and an exponentially temperature-dependent viscosity, respectively.

In the range of a positive separation ratio ψ, we find, as a function of ψ, for larger values of the viscosity contrast, a discontinuous change in the critical Rayleigh number as well as in the critical wavelength of the convection rolls, in contrast to their continuous behavior in the range of a constant viscosity and small values of the viscosity contrast.

The strongest qualitative influence of an exponentially dependent viscosity at the onset of convection is found in the range of negative values of the separation ratio ψ. In molecular binary mixtures, for $\psi < 0$, below the onset of convection, the minor and heavier component of the fluid mixture is, via the Soret effect, enriched near the lower and warmer boundary. In geophysical applications, where also double-diffusive models are applied, the Soret effect does not play a very strong role, but due to gravitation, the heavier minor component of the mixture is similarly accumulated in the lower warmer range of the convection layer [52,53]. For molecular binary fluids, such as water-alcohol mixtures, it is common that in closed convection cells, one has an oscillatory onset of convection in the range $\psi < 0$. However, beyond the threshold, the concentration gradient is quickly reduced by the convective motion, which soon leads to a stationary convection pattern again [31]. In the case of an exponentially temperature-dependent viscosity of the binary mixture, we find in the range $\psi < 0$ the surprising effect that, with increasing values of the viscosity contrast, already the onset of convection changes from an oscillatory to a stationary one and that the range $\psi < 0$, in which the onset of convection is still oscillatory, shrinks with increasing viscosity contrasts. According to this result for closed convection cells, we expect also in model

systems, where one has nonvanishing currents of the minor component through the lower boundary [27,45] and that are of importance for geophysical situations, a stationary onset of convection.

ACKNOWLEDGMENT

We are grateful to Georg Freund for instructive discussions about how to implement the Galerkin method in an efficient way.

[1] M. Lappa, *Thermal Convection: Patterns, Evolution and Stability* (Wiley, New York, 2010).
[2] P. Ball, *The Self-Made Tapestry: Pattern Formation in Nature* (Oxford University Press, Oxford, 1998).
[3] D. L. Turcotte and G. Schubert, *Geodynamics* (Cambridge University Press, Cambridge, 2002).
[4] *Mantle Dynamics*, edited by D. Bercovici (Elsevier, Amsterdam, 2009).
[5] F. H. Busse, in *Mantle Convection: Plate Tectonics and Global Dynamics*, edited by W. R. Peltier (Gordon and Breach, Montreux, 1989), pp. 23–95.
[6] A. Davaille and A. Limare, in *Mantle Convection*, edited by D. Bercovici (Elsevier, Amsterdam, 2009), p. 89.
[7] R. A. Houze, *Cloud Dynamics* (Academic Press, New York, 1994).
[8] B. Stevens, Annu. Rev. Earth Planet Sci. **33**, 605 (2005).
[9] M. C. Cross and P. C. Hohenberg, Rev. Mod. Phys. **65**, 851 (1993).
[10] M. C. Cross and H. Greenside, *Pattern Formation and Dynamics in Nonequilibrium Systems* (Cambridge University Press, Cambridge, 2009).
[11] J. K. Platten and L. C. Legros, *Convection in Liquids* (Springer, Berlin, 1984).
[12] E. Palm, J. Fluid Mech. **8**, 183 (1960).
[13] O. Jensen, Acta Polytech. Scand. **24**, 1 (1963).
[14] K. E. Torrance and D. L. Turcotte, J. Fluid Mech. **47**, 113 (1971).
[15] J. R. Booker and K. C. Stengel, J. Fluid Mech. **86**, 289 (1978).
[16] K. C. Stengel, D. S. Oliver, and J. R. Booker, J. Fluid Mech. **120**, 411 (1982).
[17] F. H. Busse and H. Frick, J. Fluid Mech. **150**, 451 (1985).
[18] D. B. White, J. Fluid Mech. **191**, 247 (1988).
[19] F. M. Richter, H.-C. Nataf, and S. F. Daly, J. Fluid Mech. **129**, 173 (1983).
[20] U. R. Christensen and H. Harder, Geophys. J. Int. **104**, 213 (1991).
[21] S. Balachandar, D. A. Yuen, D. M. Reuteler, and G. S. Lauer, Science **267**, 1150 (1995).
[22] P. Tackley, J. Geophys. Res. **101**, 3311 (1996).
[23] S. Androvandi *et al.*, Phys. Earth Planet. Inter. **188**, 132 (2011).
[24] J. S. Turner, *Buoyancy Effects in Fluids* (Cambridge University Press, Cambridge, 1973).
[25] H. E. Huppert and J. S. Turner, J. Fluid Mech. **106**, 299 (1981).
[26] E. Giannandrea and U. R. Christensen, Phys. Earth Planet. Inter. **78**, 139 (1993).
[27] A. Manglik, J. Wicht, and U. R. Christensen, Earth Plant. Sci. Lett. **289**, 619 (2010).
[28] T. Trümper, M. Breuer, and U. Hansen, Phys. Earth Plant. Int. **194**, 55 (2012).
[29] H. R. Brand, P. C. Hohenberg, and V. Steinberg, Phys. Rev. A **30**, 2548 (1984).
[30] W. Hort, S. J. Linz, and M. Lücke, Phys. Rev. A **45**, 3737 (1992).
[31] M. Lücke *et al.*, in *Evolution of Spontaneous Structures in Dissipative Continuous Systems*, edited by F. H. Busse and S. C. Müller (Springer, Berlin, 1998).
[32] M. C. Cross and K. Kim, Phys. Rev. A **37**, 3909 (1988).
[33] E. Knobloch and D. R. Moore, Phys. Rev. A **37**, 860 (1988).
[34] W. Schöpf and W. Zimmermann, Europhys. Lett. **8**, 41 (1989).
[35] W. Schöpf and W. Zimmermann, Phys. Rev. E **47**, 1739 (1993).
[36] R. Cerbino, S. Mazzoni, A. Vailati, and M. Giglio, Phys. Rev. Lett. **94**, 064501 (2005).
[37] B. Huke, H. Pleiner, and M. Lücke, Phys. Rev. E **78**, 046315 (2008).
[38] G. Donzelli, R. Cerbino, and A. Vailati, Phys. Rev. Lett. **102**, 104503 (2009).
[39] M. Glässl, M. Hilt, and W. Zimmermann, Eur. Phys. J. E **32**, 265 (2010).
[40] F. Winkel *et al.*, New J. Phys. **12**, 053003 (2010).
[41] M. Glässl, M. Hilt, and W. Zimmermann, Phys. Rev. E **83**, 046315 (2011).
[42] L. D. Landau and E. M. Lifshitz, *Course of Theoretical Physics, Vol. 6: Fluid Mechanics* (Butterworth, Boston, 1987).
[43] J. K. Platten, J. Appl. Mech. **73**, 5 (2005).
[44] J. Tanny and V. A. Gotlib, Int. J. Heat Mass Transfer. **38**, 1683 (1995).
[45] A. Mambole, G. Labrosse, E. Tric, and L. Fleitout, Stud. Geophys. Geod. **48**, 519 (2004).
[46] C. V. Raman, Nature **11**, 532 (1923).
[47] R. H. Eweell and H. Eyring, J. Chem. Phys. **5**, 726 (1937).
[48] R. M. Cleber and F. H. Busse, J. Fluid Mech. **65**, 625 (1974).
[49] C. Canuto, M. Hassaini, A. Quarteroni, and T. Zang, *Spectral Methods in Fluid Dynamics* (Springer-Verlag, Berlin, 1987).
[50] W. Pesch, Chaos **6**, 348 (1996).
[51] M. Kameyama, H. Ichikawa, and A. Miyauchi, Theor. Comput. Fluid Dyn. **27**, 21 (2013).
[52] M. I. Shliomis and B. L. Smorodin, Phys. Rev. E **71**, 036312 (2005).
[53] B. L. Smorodin, B. I. Myznikova, and J. C. Legros, Phys. Fluids **20**, 094102 (2008).